

## Chemical Structure of Preinhibitin in Citrus Against Citrus Stem-End Rot

Yasuo Homma, Tomihiko Ohsawa, Yutaka Arimoto, and Hiroharu Takahashi

First, second, and third authors: RIKEN (The Institute of Physical and Chemical Research), 2-1 Hirosawa, Wako, Saitama, 351-01 Japan; and fourth author: National Institute of Agro-Environmental Sciences, Ministry of Agriculture, Forestry and Fishery, Yatabe-Machi, Tsukuba, Ibaraki 305 Japan.  
Accepted for publication 7 October 1991.

## ABSTRACT

Homma, Y., Ohsawa, T., Arimoto, Y., and Takahashi, H. 1992. Chemical structure of preinhibitin in citrus against citrus stem-end rot. *Phytopathology* 82:310-314.

When pedicels of Satsuma mandarin fruits on trees were inoculated with *Diaporthe citri* and then harvested in early December and stored at room temperature, stem-end rot was not observed until late February. Numerous crystals were distributed in the tissues around the stem button. The dissolved crystals inhibited conidial germination and germ-tube elongation of *D. citri*. The substance, referred to as the preinhibitin, was hydrolyzed by refluxing in ethyl alcohol-hydrochloric acid, 10:1, for 18

h. The resinous material obtained from the ether-soluble fraction was purified by repeated preparative thin-layer chromatography on silica gel to yield pale yellow crystals. This compound was identified as a flavanone, hesperetin. The original compound proved to be a glycoside with hesperetin as the aglycon. The preinhibitin was identified as hesperetin-7-rhamnoglucoside or hesperidin.

*Additional keywords:* Citrus unshiu.

Abundant rainfall during the period of fruit development (June to September in Japan) is conducive to diseases of citrus caused by the rainborne pathogens *Diaporthe citri* F. A. Wolf (melanose), *Elsinoe fawcettii* Bitancourt & Jenk., and *Xanthomonas campestris* pv *citri*. These pathogens infect fruits or young leaves and may cause considerable injury to fruit rinds, thereby resulting in serious economic losses. However, there are certain necessary environmental conditions for these infections. For example, *D. citri* requires precipitation of 10 mm or more and high humidity at 20 C or higher, lasting for 12 h or longer (9). These pathogens only damage the rinds of the fruits and will not rot the fruits on the trees. Citrus trees possess certain inhibitory substances in their fruits and leaves (6,7) and also produce a phytoalexin, scoparone (2,3). These substances can potentially inhibit the penetration of pathogens into the fruits. Once *D. citri* has penetrated into the pedicel of the fruits, it can remain latent for a long period (up to 9 mo) (10). Citrus should have a preinhibitin within the stem-end of the fruits, so *D. citri* cannot penetrate the preinhibitin (PI) barrier and spread within fruits. Homma et al (8) demonstrated that *D. citri* could develop within the fruits near the end of storage.

This paper describes inhibitory activities and the chemical structure of the preinhibitin distributed in the fruit stem end.

## MATERIALS AND METHODS

Materials for scanning electron microscopy (SEM) were obtained from healthy, mature Satsuma mandarin (*Citrus unshiu* Markovich) fruits. The sample was a stem end with a pedicel cut longitudinally. All samples were attached to specimen stubs with silver-conducting paint and then coated with thin films of carbon and gold under high vacuum. The samples were observed and photographed under a scanning electron microscope (JSM-U3, JEOL Co., Tokyo, Japan) at 5 kV.

A stem button of tissue under the disk (7 mm in diameter and 8 mm in depth) was removed from a stem end of healthy fruit (*C. unshiu*). The tissue was cut longitudinally. It was kept on a slide glass in a petri dish and fixed with formalin-immersed filter paper. The formalin vapor sterilized the tissue, and it was dried for 30 min under high vacuum. SEM disclosed numerous

chestnut burrlike colonies of needle crystals around the central part of the underside of the abscission zone of the tissues under disk. One of the colonies was taken off with a pin, pressed on a specimen stub to make a thin film, and analyzed by Fourier-Transform Infrared Spectrophotometer (FT-IR) (Horiba Model FT-530, HORIBA, Ltd., Tokyo, Japan).

**Extraction of the crystalline substance.** Stem buttons and tissues under disks (108 samples, 7 mm in diameter and 8 mm in depth) were removed from the stem end of healthy fruits (*C. unshiu*) (Fig. 1) and separately extracted with 5 ml of acetone per stem button or tissue under disk for 7 days. Each extract was evaporated, dissolved in 3 ml of methanol, and allowed to stand for 7 days. The methanol fractions had maximum absorbance at 283 nm. All the methanol fractions from each of the 108 stem buttons and tissues under disks were measured at 283 nm and combined separately. The methanol fractions were evaporated separately and vacuum-dried in a desiccator for 24 h. The dry weights of the pooled extracts were 677 mg (stem buttons) and 2,016 mg (tissues under disks). For the first step, they were dissolved in 230 ml of methanol, concentrated to 20 ml, and allowed to stand for 6 h at 5 C for crystallization. The suspensions were filtered, and the first set of crystals were obtained from extracts of both tissues. The mother liquors were treated as above for 24 h at 5 C, and the second set of crystals were collected by filtration. The third set of crystals was collected from the mother liquors after 48 h at 5 C. The combined crude crystals of the first, second, and third crops were recrystallized from methanol, and the dry weights were determined.

After two cycles of crystallization and filtration by the above procedure, 89.9 mg of crystals from stem buttons and 309 mg from tissues under disks were obtained. Filtrates-1, -2, and -3 from each step were combined and concentrated to 50 ml. The concentrated filtrate was diluted with 50 ml of distilled water and allowed to stand for 48 h to confirm that there was no more appearance of crystalline substances.

**Measurement of tissue volumes in the fruit stem ends.** Each of 12 stem buttons and tissues under the disks were placed in a 25-ml graduated cylinder containing 10 ml of distilled water. The total volumes of 12 samples were recorded from the change in the water level in the cylinder, and an average volume was calculated.

**Inhibitory activity of crystalline substance on *D. citri* germination.** The aqueous solutions of purified crystalline substance were

prepared to the concentrations of 125, 250, 500, 1,000, and 2,000  $\mu\text{g}/\text{ml}$ . The fungus used in this study was *D. citri* cultured on sterilized citrus twigs at 25 C for 1 mo. A suspension of *D. citri* spores at a concentration of  $2 \times 10^6$  spores per milliliter was prepared with 5% aqueous fructose as nutrition for germination. After equal volumes of the above samples of inhibitor and spore suspensions were combined and mixed, then three drops of each mixture were placed on a sterile glass slide in a moist, sterile petri dish, and incubated at 25 C for 24 h. Five hundred or more of total spores per each mixture were observed under a light microscope. Inhibition (%) ( $x$ ) was calculated by the following equation:  $x =$

$$\left(1 - \frac{\text{number of germinated spores}}{\text{number of total spores}}\right) \times 100.$$

## RESULTS

**Presence of crystals around stem-end core of citrus fruits.** The central core of a longitudinally sectioned stem button and the tissue under the disk from a healthy fruit at a mature stage is shown in Figure 2. Figure 2A shows the abscission layer (A) of the disk and its surrounding tissue. The upper side is a disk, and the lower side shows a tissue under the disk. Figure 2B is a close-up picture of the vascular bundle in the upper side of the abscission zone. In the vascular bundles, parasitized by the pathogen (8), a few crystals were observed (Fig. 2B), and a few crystals were sometimes observed inside of the disk. In contrast, numerous crystals were observed around vascular bundles in the tissues under the disk and the lower side of the abscission zone (Fig. 2C). It was observed that the tissues under the disks had more crystals than the disks.

The results obtained by the extraction experiment in stem buttons and tissues under the disks in citrus stem end are shown in Table 1. The dry weights of total extracts were 677.3 mg from stem buttons and 2,016.5 mg from tissues under the disks. Net crystalline substances were 89.9 mg (96.0 mg by UV determination) from stem buttons and 309.0 mg (474.7 mg by UV determination) from tissues under the disks.

Based on the measurement of a stem button and the volume of a tissue under the disk, the concentrations of inhibitory substance per stem button and tissue under the disk were 9.9 and 14.0 mg/ml, respectively. The latter's concentration was 1.4 times higher than the former.

**Inhibition of *D. citri* pycniospore germination by crystals from tissues under disks.** The purified crystal solutions were tested for inhibition (Table 2). At concentrations of 63  $\mu\text{g}/\text{ml}$ , the germination of 63% of spores of *D. citri* was inhibited; further inhibition increased as the concentration of the crystal solutions increased.

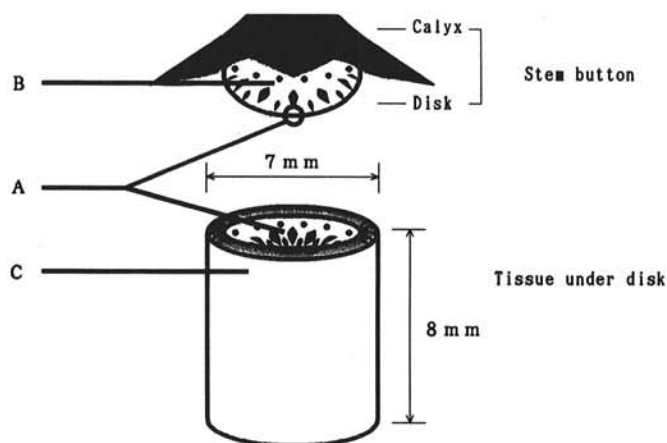


**Fig. 1.** The diagram of the stem button and the tissue under disk for extraction of inhibitory substances. A, B, and C show the positions in the photograph of scanning electron microscopy in Figure 2.

Concentrations higher than 250  $\mu\text{g}/\text{ml}$  almost completely inhibited pycniospore germination of *D. citri*. The inhibitory activities of purified crystal solutions were similar to those of authentic hesperidin.

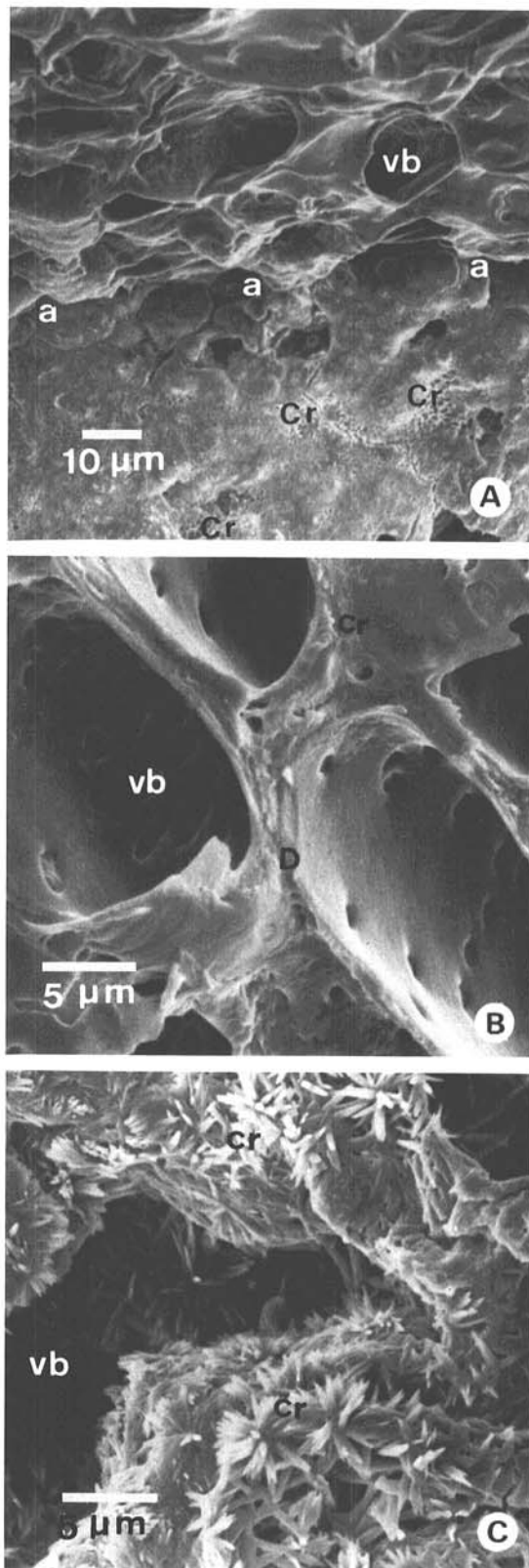


**Fig. 2.** Longitudinally cut stem-end of Satsuma mandarin fruits at matured stage in November. A, B, and C in Figure 2 correspond to A, B, and C in Figure 1. A, disk (upper half above the abscission zone [a]) and tissue under the disk (lower half under the abscission zone). Crystals (Cr) are growing mostly in tissue under the disk. B, crystals (Cr) are few in the inside of disk (D) in stem button. C, tissue under the disk is covered with crystals (Cr). vb = Vascular bundle.

The active compound was isolated as a white powder, mp 258.5–264 C, soluble in aqueous sodium bicarbonate, methanol, or dimethyl sulfoxide (DMSO) and insoluble in diethyl ether or benzene. The IR (KBr) spectrum showed broad, strong bands due to hydroxyl group(s) (3,600–3,000  $\text{cm}^{-1}$ ) and a set of strong bands (1,638 and 1,600  $\text{cm}^{-1}$ ) attributable to a conjugated carbonyl group.

The H-NMR spectrum ( $\delta$ , ppm in DMSO- $d_6$ ) indicated the presence of acidic protons ( $\delta$  12.0, 9.1), two independent groups of aromatic protons with coupling among each group ( $\delta$   $\approx$ 6.9,  $\delta$   $\approx$ 6.1), and several signals attributable to protons attached to carbons bonded with oxygen ( $\delta$  4.4–5.5, 3.1–3.8) including a ethoxyl group ( $\delta$  3.8) and a doublet methyl group ( $\delta$  1.1). The presence of acidic protons, two groups of aromatic protons, and an unsaturated carbonyl group suggested the existence of a flavonoid structure (12). UV absorption (283, 325  $\text{nm}^{-1}$ ) also supported this conjecture. The highly polar character ( $R_f$  = 0.3 and 0.47 on silica gel thin-layer chromatography (TLC), developed by ethyl ether and ethyl acetate:methyl ethylketone-formic acid water, 5:3:1:1, respectively) as well as the presence of many CH-O protons in the NMR spectrum are best explained by a glycosidic structure.

A preinhibitin sample (239 mg) was hydrolyzed in refluxing ethyl alcohol (EtOH, 99.5%) hydrochloric acid (HCl) (10:1) for 18 h (4). The ether-soluble fraction of the product yielded 173 mg of resinous substance, which was purified by repeated preparative TLC on silica gel (n-hexane-ethyl acetate = 1:1, then  $\text{CH}_2\text{Cl}_2$ ), giving 22 mg of the aglycon in the form of pale yellow crystals, mp 215–218 C. The IR (KBr) spectrum showed one sharp band (3,480  $\text{cm}^{-1}$ ), a broad band (3,300–1,800  $\text{cm}^{-1}$ ) attributable to hydroxyl group(s), and a set of strong bands due to conjugated carbonyl groups (1,630, 1,570  $\text{cm}^{-1}$ ). This compound was positive (black-violet) in the phenol test ( $\text{FeCl}_3/\text{DMSO}$ ) (11). The NMR spectrum (500 MHz, DMSO- $d_6$ ) of the aglycon included the following signals, indicating the partial structures listed below:  $\text{CHCH}_2\text{C}=\text{O}$  (2.700, d.d.,  $J_1 = 17.15$  Hz,  $J_2 = 3.08$  Hz; 3.180, d.d.,  $J_1 = 17.15$  Hz,  $J_3 = 12.31$  Hz; 5.423, d.d.,  $J_3 = 12.31$ ,  $J_2 = 3.08$  Hz), aromatic H (5.871, d.,  $J_4 = 2.2$  Hz; 5.887, d.,  $J_4 = 2.2$  Hz), aromatic H (6.871, d.d.,  $J_5 = 1.8$  Hz,  $J_6 = 8.4$  Hz; 6.927, d.,  $J_5 = 1.8$  Hz; 6.993, d.,  $J_6 = 8.4$  Hz),  $\text{OCH}_3$  (3.775), and phenolic OH (12.1).

The absence of signals in the  $\delta$  1–2 ppm region suggested the aromatic character of this compound. Considering the 16 carbons involved in the NMR spectrum, the parent peak ( $M^+$ , mass-to-

charge ratio [ $m/z$ ] = 302) in the mass spectrum (electron impact, direct inlet) is assigned to  $\text{C}_{16}\text{H}_{14}\text{O}_6$ . As a natural phenolic compound with two benzene rings and a conjugated carbonyl group, a flavanone structure was postulated for the aglycon, and finally it was concluded that all the data stated above were best explained by the structure of a natural flavanone, hesperetin (1) (Fig. 3)

The aglycon corresponded with authentic hesperetin by TLC on silica gel ( $\text{CH}_2\text{Cl}_2 \times 5$ ) as well as by melting point (mp), infrared (IR), NMR, and mass spectroscopy (MS) analyses.

Thus, the original compound, preinhibitin, seemed to be a glycoside with hesperetin as the aglycon moiety. One of the glycosides with hesperetin as the aglycon is hesperidin (hesperetin-7-rhamnoglucoside) (Fig. 3), which is commonly found in citrus species (5). The preinhibitin was then compared with the authentic hesperidin by TLC, mp, IR, NMR, and MS (secondary ion mass spectrometry,  $M^+ = m/z$  611) analyses, and thereby unambiguously identified.

Figure 4 shows the SEM image of the central part under a disk. SEM revealed the existence of chestnut burrlike colonies (CbC), which consisted of needle crystals in the center under the abscission zone of the stem end (around Fig. 1C).

Figure 5 shows the FT-IR spectrum of a chestnut burrlike colony tissue preinhibitin. The FT-IR spectrum of the preinhibitin tissue is almost superimposable on that of the authentic hesperidin. It can be conclusively stated that needle crystals observed by SEM are those of hesperidin.

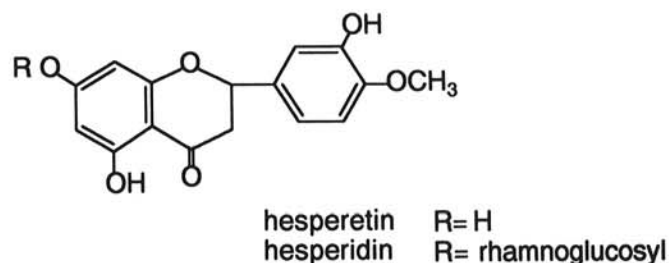


Fig. 3. Chemical structures of hesperetin and hesperidin.

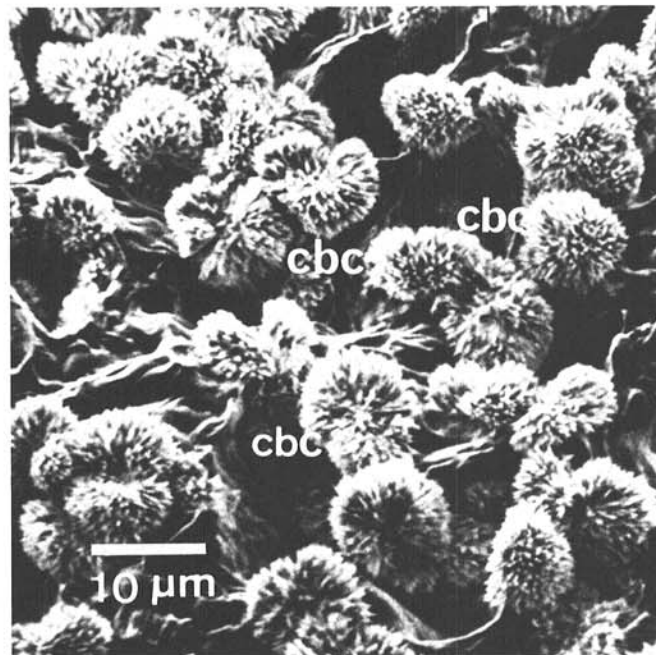


Fig. 4. Longitudinally cut tissue under a disk of Satsuma mandarin fruit at matured stage. CbC = chestnut burrlike colonies consisting of needle crystals.

TABLE 1. The amount of extract and inhibitory substance from tissues in the stem end of *Citrus unshiu* fruits<sup>a</sup>

Tissues for extraction	Dry weight (mg)		Yield (%) of inhibitory substance per total extract
	Total extract	Inhibitory substance	
Stem buttons <sup>b</sup>	677.30	89.90	13.3
Tissues under disks <sup>b</sup>	2,016.50	309.00	15.3

<sup>a</sup>Picked on 19–21 November 1989.

<sup>b</sup>One hundred eight stem buttons and 108 tissues under disks were used for extraction.

TABLE 2. Effect of preinhibitin or authentic hesperidin on conidial germination of *Diaporthe citri*

Concentration of compounds ( $\mu\text{g/ml}$ )	Inhibition of conidial germination (%)	
	Preinhibitin	Authentic hesperidin
1,000 <sup>a</sup>	100	100
500	99	99
250	98	95
125	88	89
63	63	59

<sup>a</sup>Each solution contained 2.5% fructose to accelerate conidial germination.



## DISCUSSION

*D. citri* infects the pedicel or fruit-bearing shoot of the host plant, but does not rot the fruit on the tree. In some districts of Japan, ripe Satsuma mandarin fruits are picked in December and stored for a long period of time. Even if the pathogen was inoculated into the pedicel any time from June to September, stem-end rot began only in February (10). After February, the stored fruits begin to decay from the stem end. To understand why the pathogen does not induce rotting of the fruit for a long period of time after inoculation, we investigated the anatomy of the tissue around the stem button.

SEM revealed the existence of hyphae in vascular bundles within disks, but no hyphae were observed under the disks. In addition, numerous crystals were found to distribute under the abscission zone. SEM also revealed that these crystals can be washed away with acetone. These phenomena stimulated us to study the chemical structure of these crystalline compounds and their physiological property.

The acetone extract of the tissues under the disks was tested for antifungal activity, revealing that the ED<sub>50</sub> value of the crude crystalline substance was 75 µg/ml for germ-tube elongation of *D. citri* (8), whereas that of the pure crystal was 50 µg/ml. The noncrystalline portion of the acetone extract displayed no inhibitory action against the conidial germination of *D. citri* (8), which means that the crystals consist of preinhibitin and might play an important role in controlling hyphal penetration through vascular bundles into the tissues under the disks.

Chemical analysis of the extracted preinhibitin suggested a flavanone glycoside structure. So the substance was hydrolyzed by refluxing in EtOH-HCl. The obtained aglycone was identified as a flavanone, hesperetin. The original compound, preinhibitin, proved to be hesperidin (hesperetin-7-rhamnoglucoside). An FT-IR spectrum of needle crystals on longitudinally sectioned tissue under the disk was found to be identical with that of the authentic hesperidin.

The inhibitory effect of authentic hesperidin on conidial germination of *D. citri* was found to be almost the same as that of extracted hesperidin.

The concentration of hesperidin in the tissue under the disk is approximately 1.4 times higher than that in the stem button and 3.5 times higher than that in the disk that vascular bundles distribute. Hesperidin seems to be localized around and under the disk. Hesperidin crystals were abundant in the central part

of the tissue under the disk and then gradually diminished. Hesperidin crystals were not observed in the vascular bundles of disks through which these pathogens gain access to the interior of fruits. However, hesperidin crystals were abundant in the vascular bundles under the abscission zone.

Hyphae were not observed in the cross over the abscission zone, which was filled with hesperidin (8). These observations are consistent with the hypothesis that the localized accumulation of hesperidin around and under the abscission zone inhibits the invasion of the hyphae to the inside of the citrus fruits.

## LITERATURE CITED

1. Arakawa, H., and Nakazaki, M. 1960. Die absolute Konfiguration der optisch activen Flavanone. Ann. Chem. 636:111.
2. Arimoto, Y., Homma, Y., and Misato, T. 1986. Studies on citrus melanose and citrus stem-end rot by *Diaporthe citri* (Faw.) Wolf. Part 4. Antifungal substances in melanose spots. Ann. Phytopathol. Soc. Jpn 52:39-46.
3. Arimoto, Y., Homma, Y., and Ohwawa, T. 1986. Studies on citrus melanose and citrus stem-end rot by *Diaporthe citri* (Faw.) Wolf. Part 5. Identification of a phytoalexin in melanose spots. Ann. Phytopathol. Soc. Jpn 52:620-625.
4. Asahina, Y., Shinoda, J., and Inubuse, G. 1928. Ueber Flavanonglucoside. Yakugakuzasshi 48. 3:207-214.
5. King, F. E., and Robertson, A. 1931. Natural glycosides. Part 3. The position of the biose residue in hesperidin. J. Chem. Soc. 86:1704.
6. Homma, Y., and Arimoto, Y. 1988. Studies on citrus melanose and citrus stem-end rot by *Diaporthe citri* (Faw.) Wolf. Part 8. Distribution of pathogen inhibitory substances in citrus tissues. Ann. Phytopathol. Soc. Jpn 54:1-8.
7. Homma, Y., Arimoto, Y., and Misato, T. 1979. Studies on citrus melanose and citrus stem-end rot by *Diaporthe citri* (Faw.) Wolf. Part 1. Effect of citrus fruit extract, sugars and organic acids contained in citrus fruit on conidial germination of *Diaporthe citri*. Ann. Phytopathol. Soc. Jpn 45:9-16.
8. Homma, Y., Takahashi, H., and Arimoto, Y. 1989. Studies on citrus melanose and citrus stem-end rot by *Diaporthe citri* (Faw.) Wolf. Part 10. Hyphal elongation of *Diaporthe citri* from citrus fruit pedicel to stem-end and behavior of inhibitins. Ann. Phytopathol. Soc. Jpn 55:131-139.
9. Homma, Y., and Yamada, S. 1969. Factors influencing infection and development of citrus melanose by *Diaporthe citri* (Faw.) Wolf. Bull.

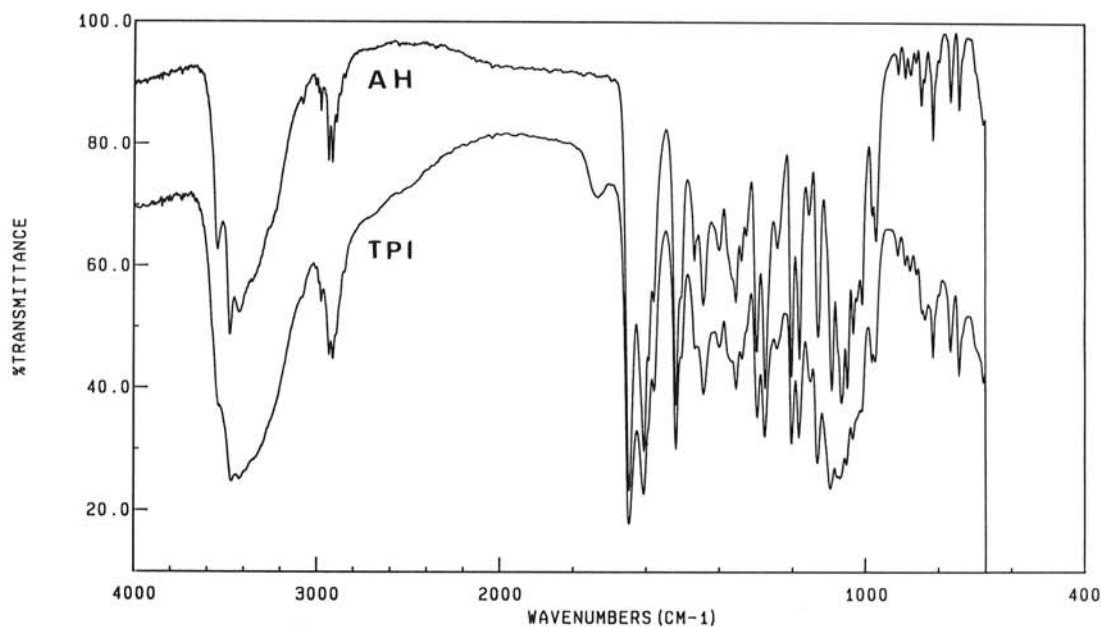


Fig. 5. The Fourier-Transform Infrared spectra of tissue preinhibitin and authentic hesperidin. TPI = tissue preinhibitin; AH = authentic hesperidin.

- Hortic. Res. Stn. B2:85-97.
10. Homma, Y., and Yamada, S. 1969. Mechanisms of infection and development of citrus stem-end rot caused by *Diaporthe citri* (Faw.) Wolf. Bull. Hortic. Res. Stn. B2:99-115.
  11. Kaneko, T., and Kubota, F., eds. 1965. Pages 933-949 in: Jikken Kagaku Koza, Supplement 5. Maruzen Co., Tokyo.
  12. Mabry, T. J., Markkam, K. R., and Thomas, M. B. 1976. The systematic identification of flavonoids. Pages 165-174 in: The Ultraviolet Spectra of Isoflavones, Flavanones and Dihydroflavonols. Springer-Verlag, New York.